Intra-Procedural MRI-Monitoring of Irreversible Electroporation of Liver Tissues in Rodent Model

Y. Zhang[1,2], Y. Guo[2], A. B. Ragin[2], R. J. Lewandowski[2,3], G-Y. Yang[3,4], G. M. Nijm[5], A. V. Sahakian[5], R. A. Omary[2,3], and A. C. Larson[2,3]

[1]Bioengineering, University of Illinois at Chicago, Chicago, IL, United States, [2]Radiology, Northwestern University, Chicago, IL, United States, [3]Robert H. Lurie Comprehensive Cancer Center, Northwestern University, Chicago, IL, United States, [4]Pathology, Northwestern University, Chicago, IL, United States, [5]Electrical Engineering and Computer Science, Northwestern University, Evanston, IL, United States

Introduction

Electroporation involves the application of a short-lived electrical field across the cell membrane to create nano-scale pores thereby increasing membrane permeability. When the electrical field across cell membrane is sufficiently strong, the pores do not reseal leading to a loss of homeostasis and eventual cell death, a process recently described as irreversible electroporation (IRE) [1]. IRE has been applied as a novel tissue ablation modality, which may offer multiple potential advantages compared to thermal treatment of hepatic lesions [2]. Finite element modeling (FEM) can be used to anticipate IRE ablation volumes; however, these methods typically assume homogeneous tissue conductivity [3] which can lead to poor approximations of the subsequent ablation volumes. MRI guidance methods have already been advocated for intra-procedural monitoring of tumor ablation procedures during thermal ablation [4]. The purpose of this study is to prospectively test the hypothesis that intra-procedural MRI can be used to immediately detect treated tissue regions during IRE procedures.

Materials and Methods

Animal Model Sprague-Dawley rats (n = 22) were used for our ACUC-approved experiments. Group A animals (4 rats) were immediately sacrificed after the MRI-monitored IRE procedure. Rats in Groups B, C and D (6 rats/group) each underwent IRE procedures with different electrode voltages applied for each group; these rats were sacrificed after 24hrs post-procedure to permit definitive formation of cell necrosis. Prior to IRE and MRI, rats were anesthetized with a high limb injection of ketamine (75-100mg/mL) and xylazine (2-6mg/mL). Rats were restrained in supine position and the left lateral lobe of the liver exposed with midline incision. Two parallel platinum-iridium needle electrodes were inserted into the center of the left lateral lobe.

MRI Measurements All experiments were performed using a 3.0T clinical MR scanner (Magnetom Trio, Siemens Medical Solutions) with 4-element carotid array coils. Electrodes remained positioned within the liver throughout the procedure but were disconnected from the function generator during MRI scans. Prior to application of the IRE pulses, localization scans were performed to identify separate imaging planes perpendicular and parallel to the electrodes. Next, we acquired pre-IRE T1-weighted (T1W) gradient recalled echo (GRE) images with repetition time/echo time (TR/TE) = 200/2.5ms, flip angle = 90°, bandwidth = 500 Hz/pixel and T2-weighted (T2W) turbo spin-echo (TSE) images with TR/TE = 3500/60ms, immediately following subsequent application of the IRE pulses, MRI measurements were repeated.

IRE Procedures After pre-IRE MRI scan, rats were removed from the scanner bore but remained fixed in supine position. Electrodes were connected to IRE function generator (ECM830). 2500V square wave pulses were applied to Group A; 1000V, 1500V and 2500V pulses were applied to Group B, C and D. The total number of pulses = 8, the duration of each pulse = 100 μs, and the interval between two pulses = 100 ms. Immediately after IRE, electrodes were disconnected and animals returned to the scanner bore for follow-up imaging measurements.

FEM Simulation We used COMSOL Multi-Physics software package, which implements the finite element method to solve partial differential equations. Our simulations closely followed those described in previous IRE studies [5]. 68.0 V/mm was considered as the threshold of IRE.

Histology and Data Analysis The animals in Groups B, C and D were euthanized 24 hours after IRE. Liver specimens were fixed in formalin and stained using hematoxylin and eosin (H&E), and were evaluated by an experienced pathologist. ImageJ (NIH) was used to manually draw a region-of-interest (ROI) circumscribing areas of cellular necrosis within each image to measure the resulting IRE ablation zone for each animal. ROIs were also drawn to measure the MRI-monitored ablation zones separately within T2W TSE and T1W GRE images by an experienced interventional radiologist who was blinded to the IRE voltage. MRI-based ablation zone measurements were evaluated with respect to both ablation zones anticipated based upon FEM simulations and ablation zones measured within corresponding histology slides.

Statistical Analysis Pearson correlation coefficients were used to determine the relationship between MRI measurements and histology-confirmed ablation zone measurements. P-values less than 0.05 were considered statistically significant.

Results

For Group A, representative T1W GRE and T2W TSE images before and immediately after application 2500V IRE pulses are shown in **Fig.1**. For Groups B, C and D, FEM-predicted ablation zones (with anticipated 68.0V/mm lethal threshold) for electrode voltages of 1000V, 1500V, and 2500V, along with corresponding post-IRE T1W GRE images with 24hrs post-procedural H&E histology images are shown in **Fig.2**. Both FEM-anticipated and MRI-monitored IRE ablation zones clearly increased in size with increasing electrode voltage. In **Fig.3**, MRI measurements were highly correlated with histology-confirmed ablation zone measurements (r = 0.88 for T1W and r = 0.92 for T2W, p < 0.001 for both).

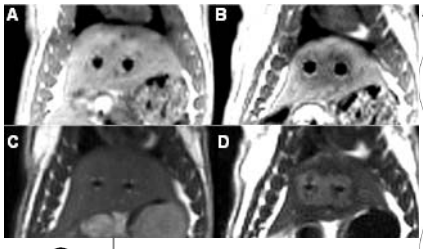

Fig.1 (Right) Representative T1W GRE (**A**, **B**) and T2W TSE images(**C**,**D**) acquired before (Pre-IRE: **A**, **C**) and immediately after (Post-IRE: **B**, **D**) the application of 2500V IRE pulses. Electrodes were depicted as signal voids. Electroporated tissues were hypo-intense within T1W GRE images (**B**) but consistently hyper-intense within T2W TSE image (**D**).

Conclusion

MRI permits immediate depiction of ablated tissue zones for intra-procedural monitoring during IRE ablation procedures. These intra-procedural measurements could potentially be used to elicit repeat application of IRE pulses or adjustments to electrode positions to ensure complete treatment of targeted lesions.

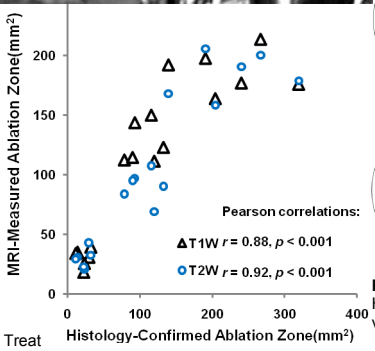

Fig.3 (Right) Scatterplots showing the relationship between intra-procedural MRI-based ablation zone measurements and histology-confirmed ablation zone measurements.

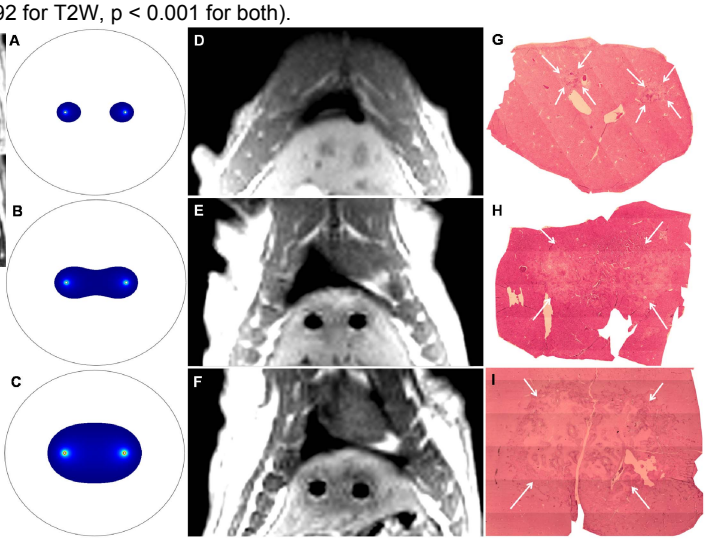

Fig.2 FEM-anticipated ablation zones (**A**-**C**), post-IRE T1W GRE images (**D**-**F**) and corresponding H&E pathology from livers harvested 24hrs post-IRE (**G**-**I**) following IRE procedures with electrode voltages of 1000V, 1500V and 2500V (top, middle, and lower rows, respectively).

Reference: [1]. Rubinsky et al. Technol Cancer Res Treat 2007;6:37-48 [2]. Ahmed et al. J Vasc Interv Radiol.2002;13:S231-244 [3]. Edd et al. Technol Cancer Res Treat 2007;6:275-286 [4]. Butts et al. JMRI. 2001;13:99-104 [5]. Miklavcic et al. Biochim Biophys Acta 2000. 1523;73-83

Acknowledgments: This work was made possible by CA134719 from National Cancer Institute and UL1 RR025741 from National Center for Research Resources (NCRR), both components of National Institutes of Health (NIH), and NIH Roadmap for Medical Research.